51st AIAA/ASME/ASCE/AHS/ASC Structures, Structural Dynamics, and Materials Conference
 18th
12 - 15 April 2010, Orlando, Florida

AIAA 2010-2860

Mixed mode in-plane fracture analysis of laminated fiber reinforced composites using the variational multiscale cohesive method

Siva Shankar Rudraraju,* Amit Salvi,† Krishna Garikipati,‡ and Anthony M. Waas §
College of Engineering, University of Michigan, Ann Arbor, MI 48109, USA

Extending our earlier work on Mode-I crack propagation presented in earlier SDM conferences, this manuscript details the research work currently underway in our group to objectively simulate mixed-mode crack propagation in laminated fiber reinforced composite materials. The analytical framework and numerical implementation using the variational multi-scale cohesive method (VMCM) is discussed. Further, mixed-mode curved crack propagation simulations and their qualitative comparison with experimental observations is presented.

I. Introduction

The increased use of laminated fiber reinforced composites as load bearing structural elements necessitates a fundamental understanding of the mechanical response, damage tolerance and damage growth in these materials. While a considerable amount of literature is present on addressing damage growth in the form of delamination crack growth, lying parallel to the interfaces of the different layers of a composite, much less is known or understood about damage propagation when a crack or damage in the form of a crack is present through the thickness of a composite structure. The influence of such wide area damage on the load bearing ability of a homogeneous and isotropic material has received considerable attention in the past; however, a similar effort at resolving issues in a non-homogeneous and macroscopically orthotropic structure is still a problem that requires resolution. Because of the different length scales associated with the microstructure of a composite material and the resulting composite structure, a multitude of failure mechanisms can be operative simultaneously, leading to a very complex picture associated with the manner in which damage progresses in a composite structure. Even though, an initial, sharp, through the thickness crack can be present in a composite structure, as soon as damage (this can be in the form of matrix micro-cracking) accumulates at the initial crack tip , crack blunting and spreading of such damage in the highly stressed areas around this initial crack occurs. When this initial crack starts to grow, a zone of material that is considerably larger than that would be found in a monolithic material, in the form of a band is seen to grow along with this crack like feature. That is, there is no clean "crack" that can be identified as in a monolithic material like metal. Instead, a diffused zone of damage is seen to advance. A large toughness is associated with this damage growth, largely influenced by the fibers that bridge the damage zone, providing additional resistance for primary crack growth. This additional resistance is very desirable and is a major contributor to the increased toughness of these laminated composites. However, inspite of all these inherent advantages of increased strength and stiffness, the applicability of these materials is often limited due to the lack of a fundamental understanding of the failure mechanics involved in these materials. Further, the numerical simulation of failure and damage propagation in these materials has proven to be a formidable excercise and the required numerical frameworks are still in their early stages.

To understand and address this complex mechanics and to circumvent the numerical limitations on objective simulation of crack propagation in materials, a micro-mechanics based, mesh independent numerical

*Graduate Student, Department of Mechanical Engineering.
†Research Fellow, Department of Aerospace Engineering.
‡Associate Professor, Department of Mechanical Engineering.
§Professor, Department of Aerospace Engineering and Department of Mechanical Engineering. Associate Fellow, AIAA.

technique for simulating crack propagation is essential. Standard finite elements fail to accomplish this task as they lack the ability to capture the discontinuous displacement modes involved in crack propagation problems. However, in recent years finite elements with discontinuities (enhanced finite elements) have gained increasing interest in modeling material failure, due to their ability to capture the specific kinematics of a displacement discontinuity(like cracks) through additional discontinuous deformation modes. In discontinuous displacement enhanced finite elements the crack path is present inside the elements, unlike cohesive zone methods which are restricted to crack propagation along element interfaces. The ability of the enhanced finite element to encompass a crack path, leads to objective simulation of crack propagation without any mesh bias. Depending on the support of the enriching discontinuous displacement modes, the enhanced finite elements are popularly known as enhanced strain finite elements (EFEM- elemental enrichment)[6,9–14] and extended finite elements (XFEM - nodal enrichment).[7,8,15,16] Interested readers are referred to Oliver et al.,[18] for detailed discussion and comparison of these methods. Though these enhanced methods provide a general numerical framework for simulation of crack evolution, the actual micromechanics implementation which incorporates the physics of crack formation is wide open. In this context, we present the Variation Multiscale Cohesive Method (VMCM), which is an enhanced finite element method containing elemental displacement field enrichment. Here the VMCM method advanced by the authors is briefly presented, and it is used to study through the thickness crack propagation in fiber reinforced laminated panels. A more detailed presentation of VMCM is available in other related studies by the authors.[1–3] Using the VMCM methodology, the numerical simulation of single edge notched three point bend specimens (SETB) of interest are presented in this work. The analysis is used to gain further understanding of mixed mode crack propagation.

The paper is organized as follows: Section II briefly discusses the experimental results which were the primary motivation for this work. Section III presents the details of VMCM numerical implementation. Thereafter, numerical simulations are provided in Section IV and they are compared against experimental observations. The concluding remarks are presented in Section V.

II. Motivation and experimental observations

Our interest in numerically simulating the experimentally observed through-the-thickness crack evolution in laminated fiber composite panels was the primary motivation for this research. The material used in all the experiments herein is a carbon fiber/epoxy $[-45/0/+45/90]_{6s}$ laminated fiber reinforced composite with a volume fraction of 0.55, and whose lamina and laminate properties are given in Table 1.

The SETB configurations used in this study are shown in Figure 1. Depending on the loading point location the specimens are classified as symmetric or eccentric loaded specimens. The symmetric loading configuration leads to a 'globally Mode-I' type crack evolution and the eccentrically loaded configuration is a good platform for understanding mixed-mode (Mode-I, Mode-II) crack evolution. SETB specimens were cut from the composite panels using water jet facility. The notch was introduced and a knife edge was used to introduce a sharp starter crack [a]. The specimens were supported on rubber rollers both at the loading and support points to minimize any local inelastic deformation. The specimens were loaded on a specially designed loading frame with anti buckling guide rods that prevents out of plane movement of the specimens. The specimens were loaded at a rate of $0.01mm/sec$ using hydraulically operated MTS testing machine and were loaded until failure. Load was measured by a load cell and the load point displacement was measured in between the top and bottom loading rollers using an LVDT. For the symmetric loading condition, five specimen sizes with geometrically scaled planar geometry and fixed thickness were considered. For the symmetric loading configuration, multiple specimens of each size were tested to significantly capture the failure response envelope. The load - load point displacement($P\Delta$) responses of these specimens are shown in Figure 6 [b]. Some of these experimental observations, including the details of how the bridging zone evolves and the related numerical simulations are explained in more detial in a recent publication by the authors.[3] Similar experiments are currently underway for eccentrically loaded specimens, and the observed curved crack evolution for some of these specimens is shown in Figure 9.

[a] In the work shown in this manuscript, the mixed-mode numerical simulations of eccentrically loaded specimens have a finite width starter crack to circumvent stress resolution issues. We are currently working on this aspect of mesh sensitivity of the numerical crack evolution.

[b] All experimental results presented herein have been normalized.

Based on these experimental observations, we identified three clear goals for our work related to numerical simulation of failure in fiber reinforced composites. The numerical platform should be capable of:

- Objective simulation of crack propagation by effectively evolving displacment discontinuities (cracks) within the finite element material domain.
- Reproducing the macroscopic load-load point displacement response of any given structure (i.e to numerically reproduce results like Figure 6).
- Simulating the crack tip, bridging zone and crack wake evolution mechanics as closely as possible to the experimentally observed failure process, and thereby being able to correctly simulate the full mixed mode crack propagation.

As matters stand, the development of the numerical method is largely complete for mixed mode crack propagation. It has succesfully simulated globally Mode-I crack experimental observations, and the results from mixed-mode (like in curved crack propagation) simulations are very encouraging. The current focus is on gaining more insights into the mechanics of mixed mode propagation (like relevant traction-separation inputs, mode-mixity conditions, etc) which are essential inputs for the numerical framework.

III. Mathematical Formulation

The standard weak form of the balance of linear momentum over the domain Ω (Figure 2) is given by,

$$\int_{\Omega} \nabla^s \boldsymbol{w} \colon \boldsymbol{\sigma} \ \mathrm{dV} = \int_{\Omega} \boldsymbol{w} \cdot \boldsymbol{b} \ \mathrm{dV} + \int_{\partial\Omega_t} \boldsymbol{w} \cdot \boldsymbol{T} \ \mathrm{dS}. \tag{1}$$

where $\boldsymbol{\sigma}$ is the stress, $\boldsymbol{w}$ is an admissible displacement variation, $\nabla^s \boldsymbol{w}$ is the symmetric gradient of the variation, $\boldsymbol{T}$ is the external traction and $\boldsymbol{b}$ is the body force.

In the standard finite element formulation of continuum mechanics, the displacements are at least C^0 continuous. But in a wide class of problems (shear banding, fiber kink banding, transverse crack formation, delamination initiation are some examples), the displacement field can be discontinuous. In such cases, the displacement field can be decomposed into continuous coarse scale and discontinuous fine scale components (Figure 3). Such a decomposition is also imposed upon the displacement variation, $\boldsymbol{w}$. The decomposition is made precise by requiring that the fine scales, $\boldsymbol{u'}$ and $\boldsymbol{w'}$, vanish outside of some region Ω', which will be referred to as the microstructural or fine scale subdomain. This decomposition is written as,

$$\boldsymbol{u} = \underbrace{\bar{\boldsymbol{u}}}_{\text{coarse scale}} + \underbrace{\boldsymbol{u'}}_{\text{fine scale}} \tag{2}$$

The corresponding scale separation in the displacement variation is given by,

$$\boldsymbol{w} = \underbrace{\bar{\boldsymbol{w}}}_{\text{coarse scale}} + \underbrace{\boldsymbol{w'}}_{\text{fine scale}} \tag{3}$$

$$\boldsymbol{u'}, \boldsymbol{w'} \varepsilon S' = \{\boldsymbol{v'} | \boldsymbol{v'} = 0 \ \ on \ \ \Omega \setminus int(\Omega')\}$$

Substituting the above decomposition into (1), and using standard arguments, the weak form can be split into two separate weak forms. One, involving the coarse scale variation, $\bar{\boldsymbol{w}}$, and the other, involving only the fine scale variation, $\boldsymbol{w'}$.

$$\int_{\Omega} \nabla^s \bar{\boldsymbol{w}} \colon \boldsymbol{\sigma} \ \mathrm{dV} = \int_{\Omega} \bar{\boldsymbol{w}} \cdot \boldsymbol{b} \ \mathrm{dV} + \int_{\partial\Omega_t} \bar{\boldsymbol{w}} \cdot \boldsymbol{T} \ \mathrm{dS}. \tag{4}$$

$$\int_{\Omega'} \nabla^s \boldsymbol{w'} \colon \boldsymbol{\sigma} \ \mathrm{dV} = \int_{\Omega'} \boldsymbol{w'} \cdot \boldsymbol{b} \ \mathrm{dV} + \int_{\partial\Omega'_t} \boldsymbol{w'} \cdot \boldsymbol{T} \ \mathrm{dS}. \tag{5}$$

This procedure results in the fine scale weak form (5), defined only over Ω' (Figure 2). This result is crucial since it lends itself naturally to the application of desired micromechanical descriptions restricted

to the microstructural region, Ω', and not the entire domain Ω. The scale separation in $\boldsymbol{u}$ is contained in $\sigma = \mathcal{C}\colon (\nabla^s \bar{\boldsymbol{u}} + \nabla^s \boldsymbol{u'})$, where $\mathcal{C}$ is the elastic stiffness tensor.

We wish to use an appropriate micromechanical law by which the fine scale solution, $\boldsymbol{u'}$, can be expressed in terms of $\bar{\boldsymbol{u}}$ and other fields in the problem. Below, we will show how such a micromechanical law can be embedded into the formulation using the weak form (5). The final step involves elimination of the fine scale displacement, $\boldsymbol{u'}$, from the problem by substituting its relation to $\bar{\boldsymbol{u}}$ in the coarse scale weak form (4). Thus, the fine scale solution does not appear explicitly; however, its effect is fully embedded in the resultant modified weak form.

We choose Ω' to contain the crack surface Γ on which $\boldsymbol{u'}$ is discontinuous. Invoking standard variational arguments, the weak form of the fine scale problem can be reduced to the following statement of traction continuity:[5]

$$[\![\boldsymbol{\sigma}\boldsymbol{n}]\!]_\Gamma = 0 \tag{6}$$

where $[\![.]\!]$ is the discontinuity in the quantity and $\boldsymbol{n}$ is the normal to the crack surface, Γ. Writing the traction on Γ in terms of components T_n and T_m along $\boldsymbol{n}$ and $\boldsymbol{m}$ respectively (Figure 2), the traction continuity condition can be expressed as,

$$T_n\boldsymbol{n} + T_m\boldsymbol{m} = \boldsymbol{\sigma}\boldsymbol{n}|_{\Gamma^-} \tag{7}$$

The traction $\boldsymbol{\sigma}\boldsymbol{n}|_{\Gamma^-}$, is determined by the macromechanical continuum formulation. The evolution of T_n and T_m is governed by the micromechanical surface law (Eqn 8). This law, which emerges at a *finite* value of traction, is related to the displacement discontinuity which is the separation between the surfaces. There are two traction laws across a planar (2D, line) surface and the displacement discontinuity $[\![\boldsymbol{u}]\!]$ can be expressed in terms of the normal opening, $[\![\boldsymbol{u}]\!].\boldsymbol{n}$, and tangential slip, $[\![\boldsymbol{u}]\!].\boldsymbol{m}$, across Γ.

We now consider a specific functional form for the micromechanical model, emerging at a non-vanishing traction,

$$T_n = T_{n_0} - \mathcal{H}_n[\![\boldsymbol{u}]\!].\boldsymbol{n}, \qquad T_m = T_{m_0} - \mathcal{H}_m[\![\boldsymbol{u}]\!].\boldsymbol{m} \tag{8}$$

where T_{n_0} and T_{m_0} are the maximum values of T_n and T_m admissible on Γ (Figure 2), $[\![\boldsymbol{u}]\!].\boldsymbol{n} > 0$ is the normal jump (Mode-I type crack opening) and $[\![\boldsymbol{u}]\!].\boldsymbol{m}$ is the tangential slip (Mode-II type crack face slip) along the elemental crack face, $\mathcal{H}_n$ and $\mathcal{H}_m$ are the softening moduli for the Mode-I and Mode-II crack opening evolution, respectively. Consistency between the micromechanical law and the macromechanical continuum description is enforced by (7) via (8).

Substituting (8) in (7) and dispensing with the explicit indication of $\boldsymbol{\sigma}\boldsymbol{n}|_{\Gamma^-}$,

$$(T_{n_0} - \mathcal{H}_n([\![\boldsymbol{u}]\!].\boldsymbol{n}))\boldsymbol{n} + (T_{m_0} - \mathcal{H}_m([\![\boldsymbol{u}]\!].\boldsymbol{m}))\boldsymbol{m} - \boldsymbol{\sigma}\boldsymbol{n} = 0 \tag{9}$$

Expanding (9) up to first order terms, in order to solve for $\boldsymbol{u'}$:

$$\begin{aligned} (T_{n_0} - \mathcal{H}_n([\![\boldsymbol{u}]\!].\boldsymbol{n}))\boldsymbol{n} + (T_{m_0} - \mathcal{H}_m([\![\boldsymbol{u}]\!].\boldsymbol{m}))\boldsymbol{m} - \boldsymbol{\sigma}\boldsymbol{n} & \\ -\mathcal{H}_n(\delta[\![\boldsymbol{u}]\!].\boldsymbol{n})\boldsymbol{n} - \mathcal{H}_m(\delta[\![\boldsymbol{u}]\!].\boldsymbol{m})\boldsymbol{m} & \\ -(\mathcal{C}\colon(\nabla\delta\bar{\boldsymbol{u}} + \nabla\delta\boldsymbol{u'}))\boldsymbol{n} &= 0 \end{aligned} \tag{10}$$

where the first line in (10) represents a zeroth-order approximation to (9), and the remaining terms are the first order corrections. Using $\boldsymbol{u'} = [\![\boldsymbol{u}]\!]C_\Gamma$, where C_Γ is the fine scale interpolation (Figure 4), converts (10) into a linear equation in $\delta[\![\boldsymbol{u}]\!]$ which can be solved, and then the incremental fine scale field is obtained from $\delta\boldsymbol{u'} = \delta[\![\boldsymbol{u}]\!]C_\Gamma$. Formally, it is represented as,

$$\delta\boldsymbol{u'} = F[\bar{\boldsymbol{u}}, \boldsymbol{\sigma}, T_n, T_m, \xi_n, \xi_m] \tag{11}$$

Extending the incremental formulation to $\boldsymbol{\sigma}$, which in a general nonlinear problem can be expanded up to first order as $\boldsymbol{\sigma} = \boldsymbol{\sigma}^{(0)} + \mathcal{C}\colon (\nabla\delta\bar{\boldsymbol{u}} + \nabla\delta\boldsymbol{u'})$, where $\boldsymbol{\sigma}^{(0)}$ is the converged value of $\boldsymbol{\sigma}$ in the previous solution increment, and substituting $\boldsymbol{u'}$ in (4), we obtain the coarse field weak form which is independent of the fine scale displacement $\boldsymbol{u'}$. On solving for $\delta\bar{\boldsymbol{u}}$, the incremental fine scale field $\delta\boldsymbol{u'}$ can be recovered via (11). Iterations are to be performed: $\bar{\boldsymbol{u}}^{(i+1)} = \bar{\boldsymbol{u}}^{(i)} + \delta\bar{\boldsymbol{u}}$, $\boldsymbol{u'}^{(i+1)} = \boldsymbol{u'}^{(i)} + \delta\boldsymbol{u'}$, until a converged solution is obtained. From (4),(10) and (11), it should be clear that the VMCM method results in an embedding of the micromechanical surface law into the coarse scale weak formulation. Interested readers are referred to[5] for a more detailed discussion of the numerical framework.

Having briefly presented the numerical formulation for mixed-mode cohesive crack evolution, we now direct our attention to simulations of through-thickness crack propagation in laminated fiber composites using this framework.

IV. VMCM Simulations

The variational multiscale implementation leads to an objective and numerically robust implementation. Interest readers are referred to[3,5] for details of the method. As discussed above, the VMCM implementation is an enhancement on the traditional variational multiscale implementations in its micromechanics implementation and application. A continuum is assumed to behave according to an appropriate constitutive law until a certain condition is satisfied which triggers fine scale computations associated with the onset of cracking. When crack growth occurs, the resulting tractions on the crack faces that arise due to fiber bridging and other mechanisms, are captured through a traction-separation law.

This implementation has two distinct advantages: (1) No a priori knowledge of crack path is required, and the entire domain is capable of propagating cracks according to the input traction-separation relations when the the crack initiation criterions are met. (2) The same element behaves as both a continuum and failure element depending upon the the physical state of its material domain. Thus, no adhoc stiffness values are required as in traditional coheize zone models (CZM). These drawbacks of traditional cohesive zone models have been clearly addressed in a recently published work.[19,20] In particular, two issues were considered; (1) when CZM is used, the placement of CZM elements along the intended crack path can lead to an alteration of the stiffness of the original body that is to be studied, and, (2) The traction-separation laws used for traditional CZM modeling, which start with a vanishing traction at vanishing separation, may be in conflict with the presence of an intense stress field that was present in the original body that is being modelled. In light of this, we would like to stress again that both these major drawbacks of CZM are circumvented in VMCM.

In the VMCM simulations, the cohesive behaviour of the material is captured through the cohesive traction separation laws given by, $T_n = T_{n_0} - \mathcal{H}_n\xi_n$, $T_t = T_{t_0} - \mathcal{H}_t\xi_t$,with subscript n denoting normal direction and t denoting tangential direction and $\mathcal{H}_n$, $\mathcal{H}_t$ are the normal and tangential softening moduli (which we refer to as the fiber-bridging moduli), is associated with the fine scale computations. T_{n_0} is the maximum normal traction admissible on Γ, which is the value of T_n corresponding to cracking condition. This linear evolution is graphically represented in Figure(5). The area under the curve is another key property, which is associated with the work of bridging tractions [c]. The work of bridging tractions, $\mathscr{G}_f$ is calculated by conventional procedures, in our case the value was obtained by analyzing the load displacement response of a standard compact tension specimen. The critical traction (T_{n_0}) is obtained from standard double notch tension specimen experiments.[4] The VMCM method is not restricted to any specific functional form of the traction separation law. Here a linear evolution law is presented as it is found to yield good agreement with experimental observations, and also because the actual shape of the traction separation law is still a topic of active research. However, linear or any other monotonic traction separation relationship is only an approximation of the actual fiber composite material response. In the real material, especially under curved crack conditions, the traction-separation evolution is much more complex as the material crack tip opening does not need to always monotonically increase. The details of such will be a part of the solution and will be dictated by the form and type of the bridging law in the crack wake. The representation of the traction evolution in cases which involve load (and separation) reversal, and possible subsequent increases

[c]The work associated with bridging traction in understood to also include the energy associated with matrix cracking

in the crack opening displacement locally is yet to be thoroughly studied. However, it is felt that any assumed traction-separation response should ensure that irrespective of the crack face opening displacement variations, the traction on the crack faces should monotonically decrease.

Moving on to the actual simulations results, Figure (6) shows the load-load point displacement response of SETB specimens of five different sizes under symmetric loading conditions. The corresponding simulations results are shown in Figure (7). Here the simulations accurately reproduce the macroscopic response of the SETB specimens when appropriate $\mathscr{G}_f$ values are used as input. These results, along with the evolving micromechanics of the bridging zone are discussed in detail in a recent publication by the authors.[3] Figure (8) shows a typical SETB specimen subjected to eccentric loading which involves both Mode-I and Mode-II evolution. The element deformation is the numerical manifestation of the crack tip opening displacement (CTOD). As the crack propagates, the elements weaken according to the assumed traction separation response, and beyond a certain critical deformation the CTOD reaches ξ_{n_0} and the corresponding element completely looses its normal stiffness. Similar is the evolution of the tangential stiffness component. The mesh may be post-processed to remove these dummy elements to visually show a clean crack propagation, void of material in the crack path as seen in Figure (8). Figure (9) shows the same simulation results in the undeformed mesh configuration allong with the highlighted crack path. Also shown in Figure (9) are the corresponding experimentally observed crack evolutions. But in these figures, the highly branched cracks on the surface layers of the laminate blur the real picture of the underlying crack evoltuion. Thus the polished specimen where the top and bottom layers of the laminate are removed is shown in Figure (10). As one can see, the simulations significantly reproduce the macrosopic evolution of the crack path. These results demonstrate the applicability of VMCM for simulating the complex crack evolution seen in fracture of laminated fiber reinforced composites.

V. Current Work

As stated above, we beleive that the numerical method has sufficiently matured to simulate full mixed-mode, complex crack path evolution. Certain issues related to crack path direction determination and mode-mixity are currently being investigated. Towards this end, we are also numerically deriving mixed-mode traction separation laws using micro-mechanical models. We expect to present these results in the next AIAA SDM conference, and will also complement these results with the study of size effects in eccentric loaded SETB tests with curved crack propagation.

References

[1]Siva S. Rudraraju, Ryan Vignes, Amit Salvi, Garikipati K & Anthony M. Waas, *"A multiscale crack path predicting computational method for laminated fiber reinforced composites"*, Proceedings of the 49th AIAA/ASME/ASCE/AHS/ASC Structures, Structural Dynamics, and Materials Conference, Schaumburg, Illinois, USA, 2008.

[2]Siva S. Rudraraju, Amit Salvi, Garikipati K & Anthony M. Waas, *"In-Plane fracture of laminated fiber reinforced composites with varying fracture resistance: experimental observations and numerical crack propagation simulations"*, Proceedings of the 50th AIAA/ASME/ASCE/AHS/ASC Structures, Structural Dynamics, and Materials Conference, Palm Springs, California, USA, 2009.

[3]Siva S. Rudraraju, Amit Salvi, Garikipati K & Anthony M. Waas, *"In-Plane fracture of laminated fiber reinforced composites with varying fracture resistance: experimental observations and numerical crack propagation simulations"*, International Journal of Solids and Structures, Volume 47, Issues 7-8, April 2010, Pages 901-911.

[4]Amit Salvi, Anthony M. Waas & Caliskan A, *"Energy absorption and damage propagation in 2D triaxially braided carbon fiber composites: Effects of in situ matrix properties"*, Journal of Materials Science, **43**, 5168-5184, 2008.

[5]Garikipati K, *"A variational multiscale method to embed micromechanical surface laws in the macromechanical continuum formulation"*, Computational Modeling in Engineering and Sciences, **3**, 175-184, 2002.

[6]F. Armero & K. Garikipati, *"An analysis of strong discontinuities in multiplicative finite strain plasticity and their relation with the numerical simulation of strain localization in solids"*, International Journal of Solids and Structures, **33**, 28632885, 1996.

[7]T.Belytschko, N. Moes, S. Usui & C. Parimi, *"Arbitrary discontinuities in finite elements"*, International Journal for Numerical Methods in Engineering, **50**, 9931013, 2001.

[8]T.Belytschko, H. Chen, J.X. Xu & K. Garikipati, *"Dynamic crack propagation based on loss of hyperbolicity and a new discontinuous enrichment"*, International Journal for Numerical Methods in Engineering, **58**, 18731905, 2003.

[9]K. Garikipati & T.J.R. Hughes ,*"A study of strain-localization in a multiple scale framework. The one dimensional problem"*, Computer Methods in Applied Mechanics and Engineering, **159**, 193222, 1998.

[10]T.C. Gasser & G.A. Holzapfel, *"Geometrically non-linear and consistently linearized embedded strong discontinuity models for 3D problems with an application to the dissection analysis of soft biological tissues"*, Computer Methods in Applied Mechanics and Engineering, **192**, 50595098, 2003.

[11]M. Jirasek, *"Comparative study on finite elements with embedded discontinuities"*, Computer Methods in Applied Mechanics and Engineering, **188**, 307330", 2000.

[12]J. Mosler & G. Meschke, *"Embedded crack vs. smeared crack models: a comparison of elementwise discontinuous crack path approaches with emphasis on mesh bias"*, Computer Methods in Applied Mechanics and Engineering, **193**, 33513375, 2004.

[13]J. Oliver & A.E. Huespe, *"Continuum approach to material failure in strong discontinuity settings"*, Computer Methods in Applied Mechanics and Engineering, **193**, 31953220, 2004.

[14]R.L. Borja & R.A. Regueiro, *"A finite element model for strain localization analysis of strongly discontinuous fields based on standard Galerkin approximation*", Computer Methods in Applied Mechanics and Engineering, **190**, 15291549, 2000.

[15]N. Moes, N. Sukumar, B. Moran & T. Belytschko, *"An extended finite element method (X-FEM) for two and three-dimensional crack modelling"*, Presented at ECCOMAS 2000, Barcelona, Spain, 2000.

[16]G.N. Wells & L.J. Sluys, *"A new method for modelling cohesive cracks using finite elements"*, nternational Journal for Numerical Methods in Engineering, **50**, 26672682, 2001.

[17]O. Nguyen, E.A. Repetto, M. Ortiz & R.A. Radovitzky, *"A cohesive model of fatigue crack growth"*, International Journal of Fracture, **110**, 351-369, 2001.

[18]Oliver J, Huespe AE & Sanchez PJ, *"A comparative study on finite elements for capturing strong discontinuities : E-FEM vs X-FEM"*, Computer methods in applied mechanics and engineering, **195**, 4732-4752, 2006.

[19]Z. H. Jin & C. T. Sun, *"Cohesive zone modeling of interface fracture in elastic bi–materials"*, Engineering Fracture Mechanics, vol 72, 1805-1817, 2005.

[20]Z. H. Jin & C. T. Sun, *"A comparison of cohesive zone modeling and classical fracture mechanics based on near tip stress field"*, International Journal of Solids and Structures, vol 43, 1047-1060, 2006.

Table 1. Lamina and laminate properties of carbon fiber/epoxy $[-45/0/+45/90]_{6s}$ laminated fiber reinforced composite.

Laminate	Lamina
E_{xx}: 51.5 GPa	E_{11}: 141 GPa
E_{yy}: 51.5 GPa	E_{22}: 6.7 GPa
G_{xy}: 19.4 GPa	G_{12}: 3.2 GPa
ν_{xy}: 0.32	ν_{12}: 0.33

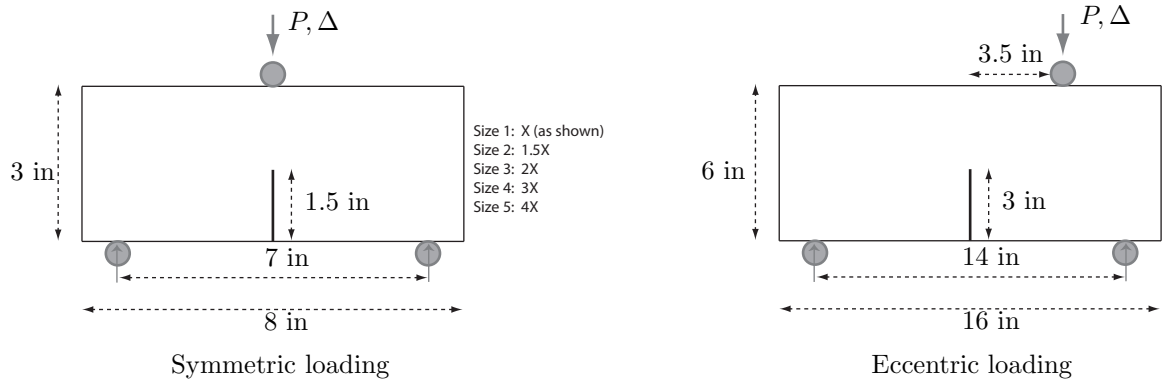

Figure 1. Single Edge Notch Bending(SETB) specimen configurations used in the crack propagation experiments. Based on the load point location, the configurations are classified as symmetric or eccentric. For symmetric specimens, size 1 has the dimensions shown in figure and other sizes are scaled versions of this base size. All specimens have a thickness of 6.35mm.

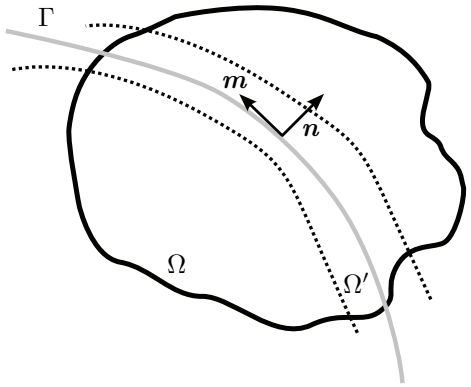

Figure 2. Decomposition of continuum body into region where coarse scale and fine scale displacements are defined. Ω is the domain of the problem, Γ is the displacement discontinuity (crack), Ω' is the support for the displacement discontinuity and n, m are the normal and tangent to Γ respectively.

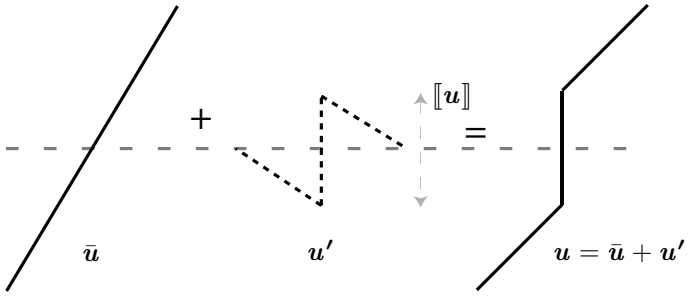

Figure 3. Schematic of scale separation. $\bar{u}$ is the coarse scale displacement field and u' is the local fine scale enhancement.

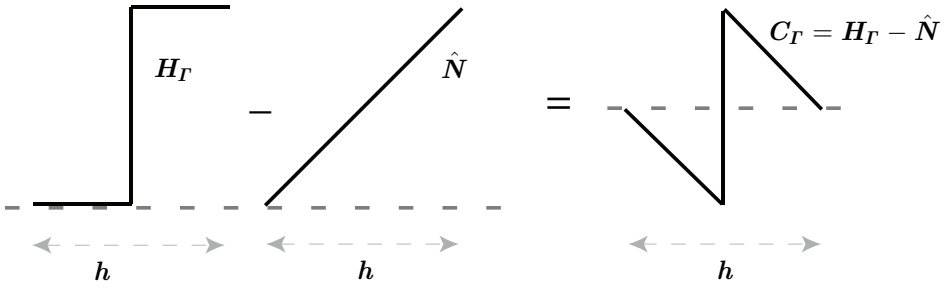

Figure 4. Discontinuous shape function used to resolve the displacement jump shown in a one-dimensional setting. It is constructed by superimposing a discontinuous function, H_Γ, on a regular polynomial, $\hat{N}$. h is the element dimension.

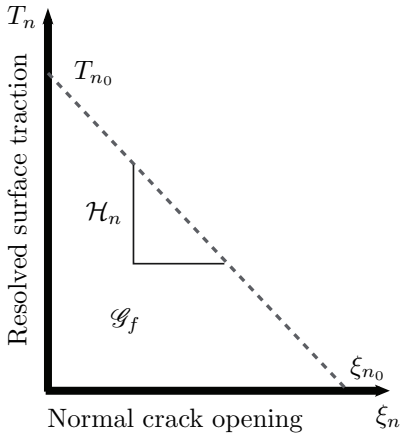

Figure 5. Linear micro-mechanical surface law for normal crack opening

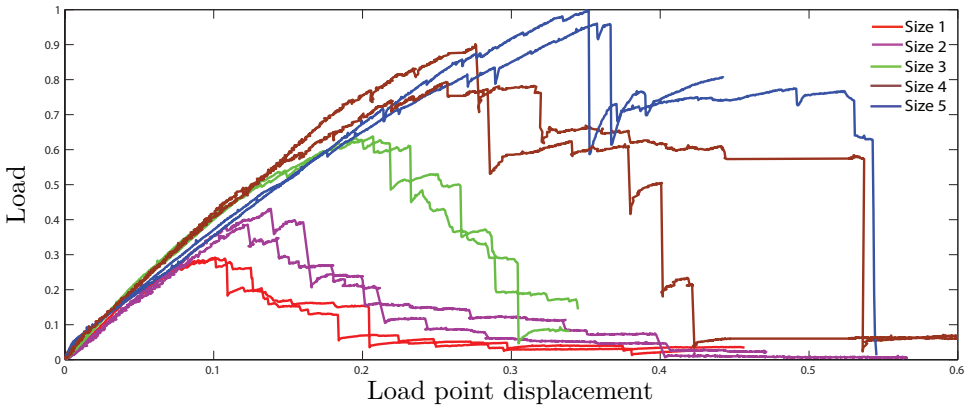

Figure 6. Experimental load-displacement curves obtained for various sizes of SETB specimens subjected to symmetric loading conditions. Multiple specimens of each size were tested to capture the envelope of the failure response.

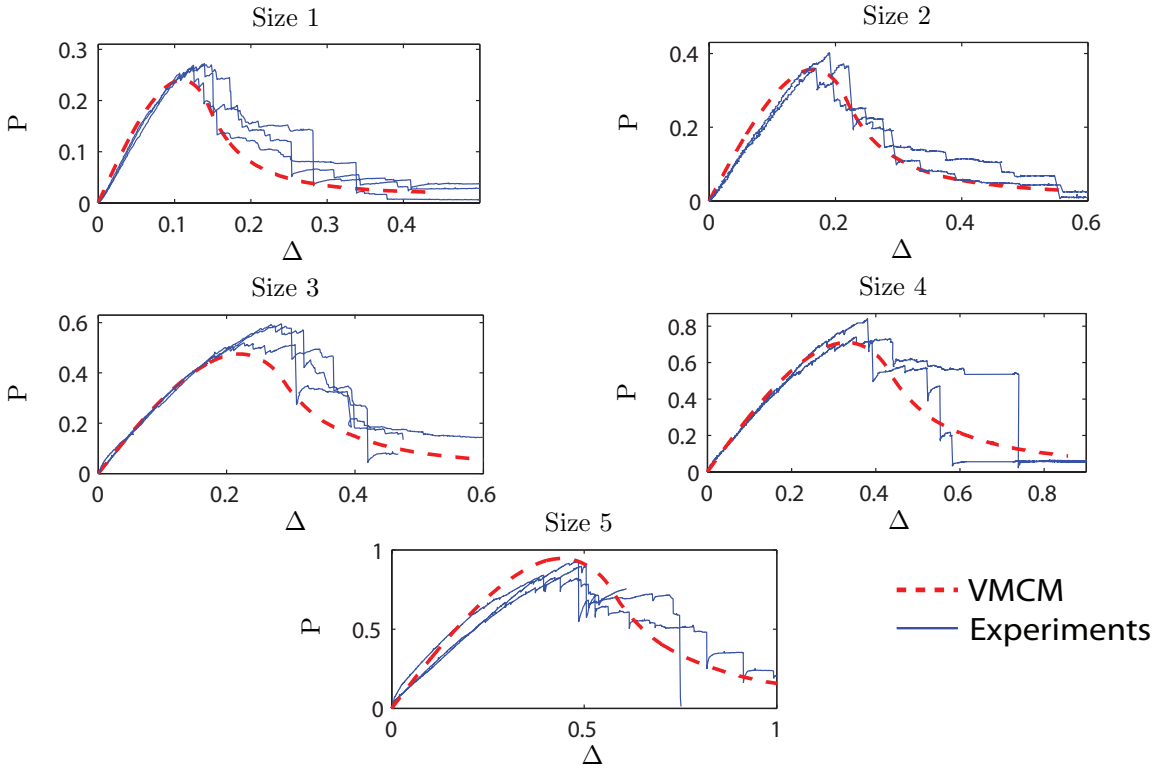

Figure 7. Load-Displacement (P-Δ) response obtained from VMCM simulations for symmetrically loaded Size 1-5 SETB specimens compared to their respective experimental curves.

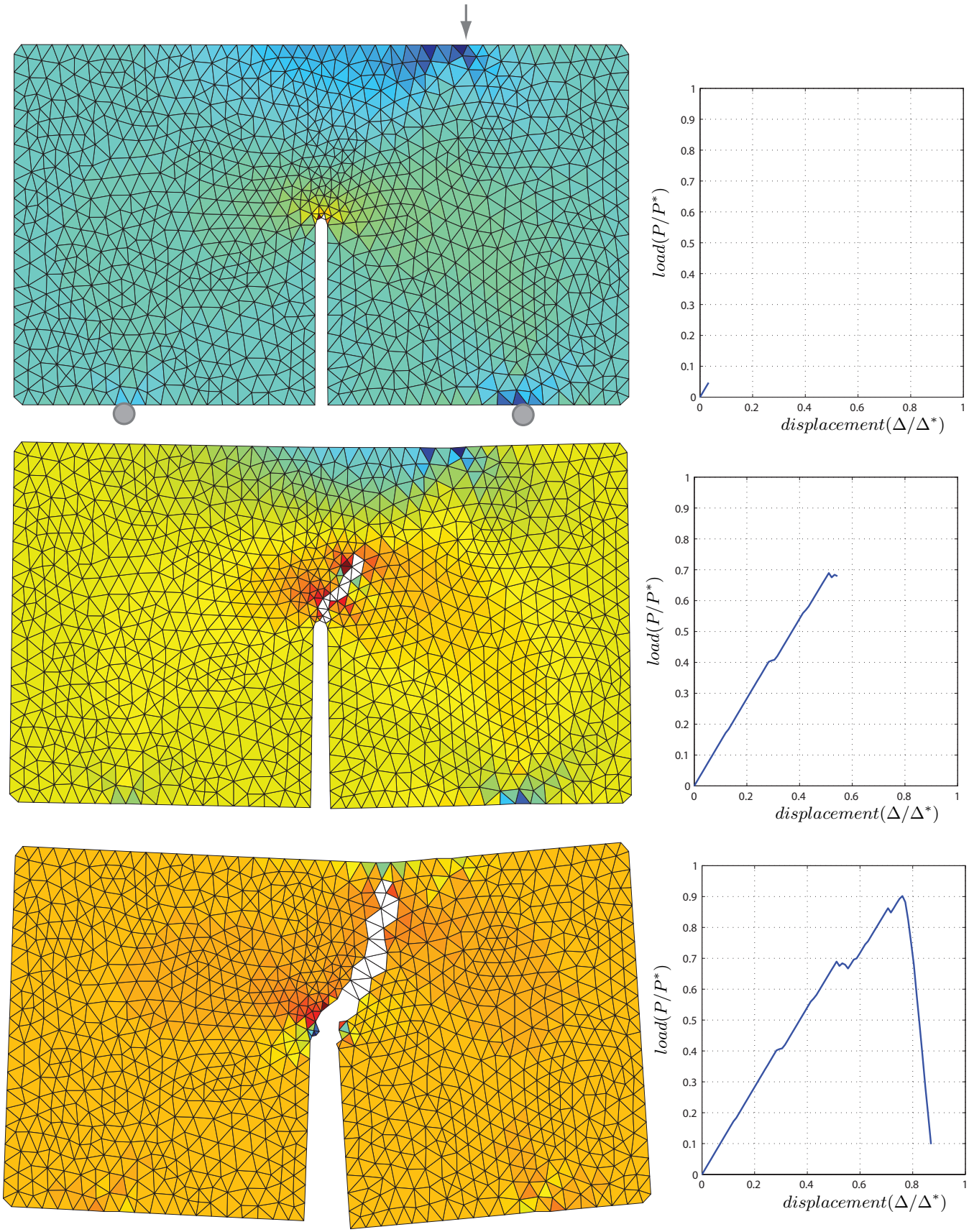

Figure 8. Deformed mesh of mixed-mode crack propagation in eccentrically loaded single edge notch three point bend (SETB) specimen and the corrresponding load-displacement response. The elements containing the crack (either bridging zone or crack wake elements) are transparent, with only their edges plotted.

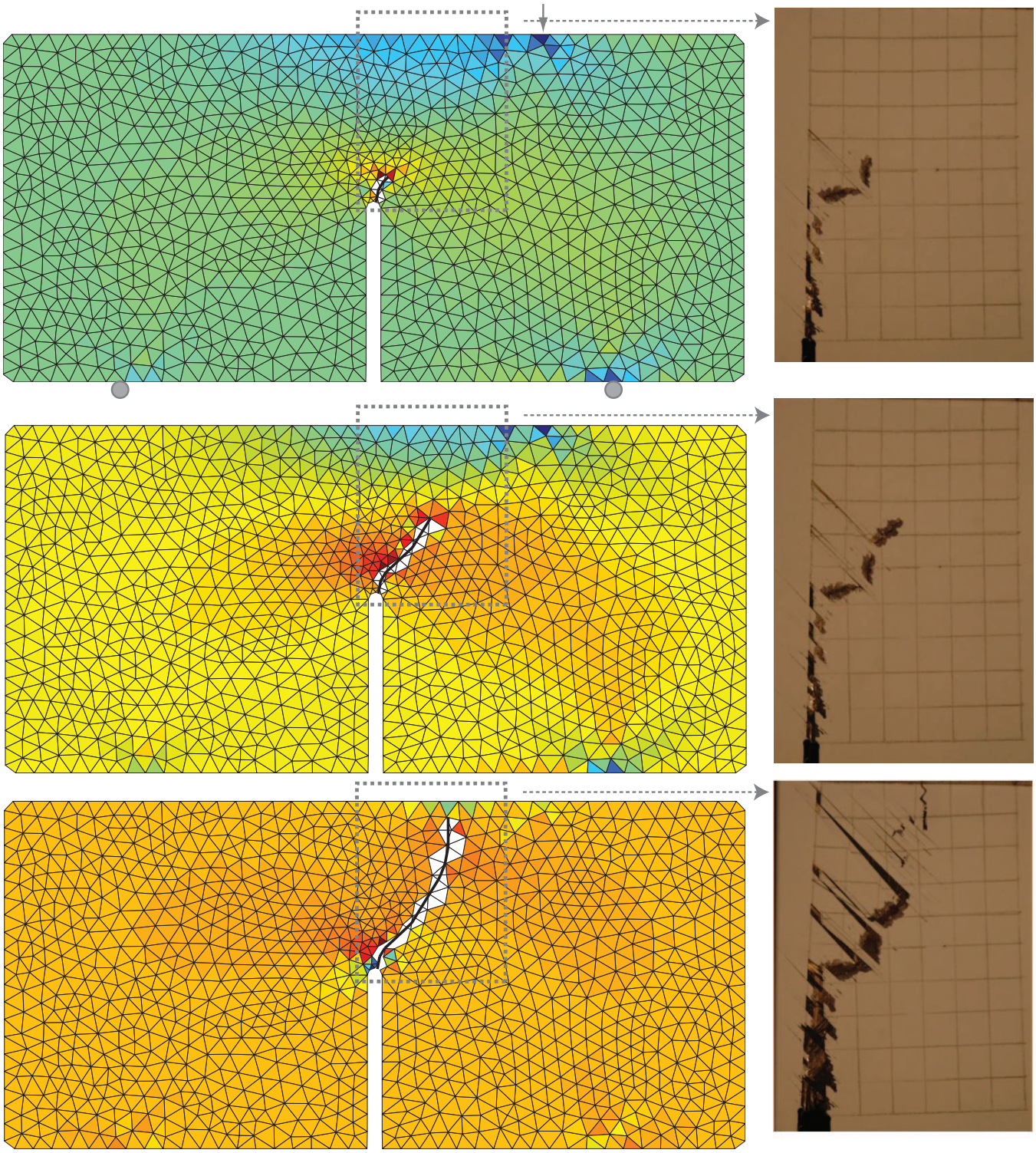

Figure 9. Undeformed mesh of mixed-mode crack propagation in eccentrically loaded single edge notch three point bend (SETB) specimen. The dark curve represents the crack path and the elements containing the crack (either bridging zone or crack wake elements) are transparent, with only their edges plotted. Shown in the inset are the corresponding experimentally observed crack paths.

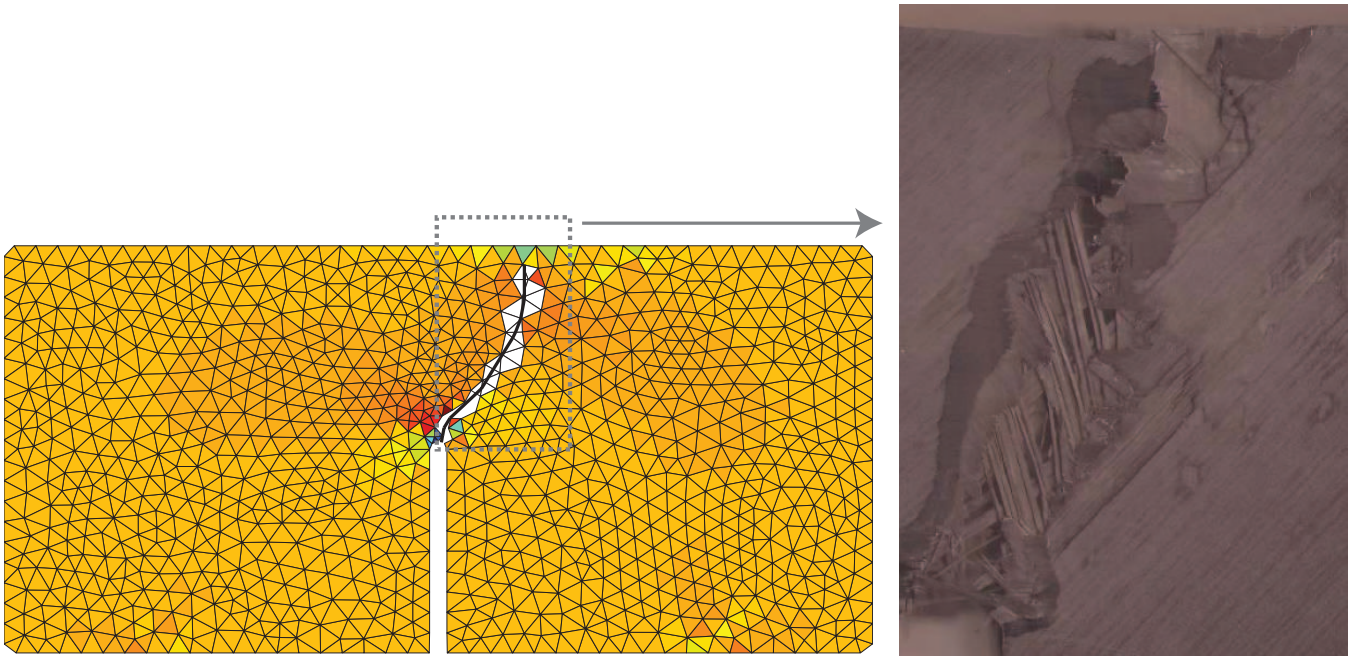

Figure 10. Comparison of numerical simulation and experimentally observed crack paths in eccentrically loaded single edge notch three point bend (SETB) specimen. Here the experimental specimen was polished after failure to reveal the underlying macroscopic crack.